Optical properties of $GaAs_{1-x}Bi_x$/GaAs quantum well structures grown by molecular beam epitaxy on (100) and (311)B GaAs substrates

M. Gunes[1], M.O. Ukelge[1], O. Donmez[2,*], A. Erol[2] , C. Gumus[3], H. Alghamdi[4], H. V. A. Galeti[5], M. Henini[4], M. Schmidbauer[6], J. Hilska[7], J. Puustinen[7] and M. Guina[7]

[1]Department of Materials Engineering, Faculty of Engineering, Adana Science and Technology University, 01250 Adana, Turkey

[2]Department of Physics, Faculty of Science, Istanbul University, Vezneciler, 34134, Istanbul, Turkey

[3]Physics Department, University of Cukurova, TR 01330, Adana, Turkey

[4]School of Physics and Astronomy, University of Nottingham, Nottingham NG7 2RD, UK

[5]Departamento de Engenharia Elétrica,Universidade Federal de São Carlos 13560-905, São Carlos, SP, Brazil

[6]Leibniz Institute for Crystal Growth, Max-Born-Strasse 2, 12489 Berlin, Germany

[7]Optoelectronics Research Centre, Tampere University of Technology, Tampere, Finland

Corresponding Author[*]: omerdonmez@istanbul.edu.tr

Abstract: In this work, the electronic bandstructure of $GaAs_{1-x}Bi_x$/GaAs single quantum well (QW) samples grown by molecular beam epitaxy (MBE) is investigated by photomodulated reflectance (PR) measurements as a function of Bi content ($0.0065 \leq x \leq 0.0215$) and substrate orientation. The Bi composition is determined *via* simulation of high-resolution X-ray diffraction (HR-XRD) measurement and found to be maximized at 2.15%Bi and 2.1%Bi samples grown on (100) and (311)B GaAs substrate. However, the simulations indicate that the Bi composition is not only limited in the GaAsBi QW layer but extends out of the GaAsBi QW towards to GaAs barrier and forms GaAsBi epilayer. PR spectra are fitted with the third derivative function form (TDFF) to identify the optical transition energies. We analyze the TDFF results by considering strain-induced modification on conduction band (CB) and splitting of the valence band (VB) due to its interaction with the localized Bi level and VB interaction. The PR measurements confirm the existence of a GaAsBi epilayer *via* observed optical transitions belong to GaAsBi layers with various Bi compositions. It is found that both Bi composition and substrate orientation have strong effects on the PR signal. Comparison between TDFF and calculated optical transition energies provides a bandgap reduction of 92meV/%Bi and 36meV/%Bi and an interaction

strength of the isolated Bi atoms with host GaAs valence band (C_{BiM}) as 1.7eV and 0.9eV for (100) and (311)B GaAs substrate, respectively.

1. INTRODUCTION

$GaAs_{1-x}Bi_x$ has been intensively studied in the last years due to its remarkable properties [1–3] and its potential applications to be used in near and mid-infrared optoelectronic as well as spintronic devices [4,5]. Replacing a small fraction of As by Bi in the host GaAs produces a large reduction in the bandgap energy of 60-90 meV/%Bi, accompanied with a rapid increase in the spin-orbit-splitting energy (Δ_{so}) [6,7]. The bandstructure of GaAsBi alloy can be determined using the valance band anticrossing (VBAC) model[8,9]. This model originally predicted that the localized Bi level affects solely valance band, while more recent studies have revealed that the CB is also affected from the localized Bi level by a 28meV/Bi%, in line with virtual crystal approximation (VCA)[6]. Moreover, since there is composition-dependent lattice mismatch between GaAs and GaAsBi, strain-induced effects on the CB and VB should also be taken into account when determining the bandstructure of GaAsBi. While GaAsBi has been widely recognized as promising for novel optoelectronic and spintronic; epitaxy of GaAsBi is not mature yet. Due to the significant difference in atomic size between As and Bi, Bi cannot be incorporated in GaAs at high growth temperatures and the quality of Bi-containing alloys is critically controlled by the As/Ga ratio, Bi/As ratio and growth temperature [10]. As it has experienced in all members of highly mismatched alloys, GaAsBi alloys have tendencies to incorporate defects, atomic cluster as well as inhomogeneities due to the unconventional growth conditions required for Bi incorporation[11–13]. These defects create localized levels above the VB and deep levels in the bandgap of GaAsBi. To improve the crystal quality, there have been some attempts[14,15]. It has been recently reported that the incorporation of a small amount of nitrogen compensates strain, resulting in enhanced crystal quality with benefit of further bandgap reduction. Furthermore, it has been reported that growing GaAsBi on GaAs with different orientations rather than [100] enhances photoluminescence (PL) intensity, but also modifies bandgap energy due to the crystal direction-dependent physical parameters such as strain, effective mass *etc*. [16,17]. However, there have been limited reports about GaAsBi epilayer grown on differently oriented GaAs substrates. Henini *et al.* and Kudrawiec *et al.* demonstrated that for the same Bi flux during MBE growth, incorporation of Bi into GaAs is larger in (311)B than in (100)-oriented GaAs substrates [18,19]. Patil *et al.* investigated multiple GaAsBi QWs grown on (411)A and (411)B GaAs and observed that both PL intensity

and Bi incorporation were enhanced in (411)A orientation at high As_4 beam equivalent pressures [20].

In this study, the electronic bandstructure of $GaAs_{1-x}Bi_x$/GaAs QW samples grown on (100) and (311)B substrate with various Bi compositions are determined by room temperature PR. HR-XRD results are used to interpret obtained optical transitions from PR spectra. The strain-included VBAC model together with VCA is utilized for calculating optical transition energies. The transition types and energies are obtained for various Bi contents and substrate orientations.

2. MATERIALS AND METHODS

2.1 Sample structure and growth procedure

We have studied six GaAsBi samples with various Bi compositions. All samples were grown by MBE at the same growth conditions to understand the effects of the substrate orientation and Bi incorporation on optical properties of the samples. Three samples were grown on semi-insulating (100) GaAs, and the others were grown on semi-insulating (311)B GaAs substrates. The growth of GaAsBi QW samples started with a 370 nm thick GaAs buffer layer. The first 300 nm was grown at 580°C with a high As overpressure; after which the growth temperature was ramped to 320°C during growth of an additional 70 nm of GaAs to enhance the incorporation of Bi in the QW. This was followed by a 10 nm thick GaAsBi QW layer and a 50 nm GaAs cap layer grown at the same temperature (see Figure 1). The growth rate was 0.4 μm/h for all layers. For efficient Bi incorporation, the atomic As/Ga flux ratio for the QW and cap layer was kept close to the stoichiometric value.

2.2 Experiments

To determine the Bi composition of the samples, HR-XRD measurements were carried out by a Bruker D8 Discover X-ray diffractometer. An asymmetric 2-bounce Ge 220 channel-cut monochromator was used to select the Cu $K\alpha_1$ line at λ = 1.54056 Å and to collimate the incident X-ray beam. From the experimental data, the change of the Bi concentration profile through the sample was determined by simulations based on dynamical scattering theory. Unfortunately, for only two samples, the XRD diffraction patterns revealed well-defined

fringes; therefore Bi compositions could be determined for only two samples, and PR measurements were utilized to determine Bi compositions for other four samples.

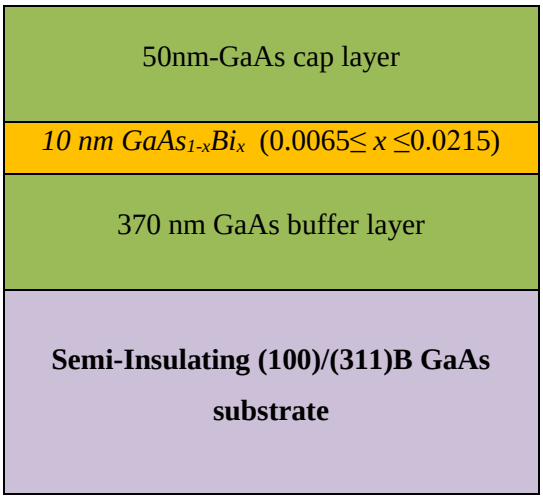

Figure 1. Nominal structure of the investigated samples

PR in the bright configuration mode was carried out by using at 650 nm diode laser as a pump source and a 100W halogen lamp as a probe source at room temperature. The laser light intensity was kept at 0.3W/cm^2. The reflected light was dispersed by a 0.5 m monochromator, and an edge filter (Newport FSQ-RG715) was placed in front of the entrance slit of the monochromator to avoid second-order of the spectrum. The signals were detected by conventional lock-in detection techniques.

2.3 Analysis method of PR results for determination of optical transition energies

PR signal was analyzed by using low electric field TDFF given as [21,22]

$$\frac{\Delta R}{R} = \sum_j C_j e^{-i\emptyset_j}\left[E - E_J + i\Gamma_j\right]^{-n_j} \quad (1)$$

where C, ∅, E, E_J and Γ are the amplitude, phase, photon energy, optical transition energy, and line-broadening, respectively. The type of critical point depending on the dimension of the structures is represented as n_j, and its values are 3 and 2.5 for the QW and bulk layers, respectively. The modulus of the individual resonance (MIR) or magnitude of the complex quantity can be obtained from Eq. 1 with the parameters taken from the fitting as

$$\Delta\rho_j = \frac{|C_j|^2}{\left[(E-E_J)^2+\Gamma_j^2\right]^{\frac{n_j}{2}}} \quad (2)$$

MIR shows the optical transition starting and finishing point. The peak position of MIR corresponds to the optical transition energy. In this study, the observed PR spectra consisted of overlap of band-to-band and localized or inhomogeneity-related transitions. In the analyzing of the localized or inhomogeneity related transition procedure, for the sake of the simplicity, n_j value is chosen as 3 or 2.5 depending on transitions in epilayer or QW. This choice slightly affects the analysis of the PR spectra and determined parameters. The details of the fitting procedure can be found elsewhere [22–24].

2.4 Theoretical model for determination of optical transition energies

To assign the optical transition energies observed in the PR spectra, we calculate the optical transition energies in GaAsBi QW structures. Since there is a lattice mismatch between GaAs and GaAsBi, in order to calculate the effect of Bi on the bandstructure of strained GaAsBi, we first determined the effect of strain on the band edge energies. To include strain-related modifications, Pikus-Bir Hamiltonian was used [28]. According to VCA, for the strained bulk GaAsBi grown on (100) GaAs, modified band-edge energies at k = 0 are given as

$$E_{CB}^{GaAs_{1-x}Bi_x}(x) = E_{CB}^{GaAs} - \alpha x + a_{CB}(\varepsilon_{xx}+\varepsilon_{yy}+\varepsilon_{zz}) \quad (3)$$

$$E_{HH}^{GaAs_{1-x}Bi_x}(x) = E_{HH}^{GaAs} + \kappa x - P_\varepsilon - Q_{\varepsilon[100]} \quad (4)$$

$$E_{LH}^{GaAs_{1-x}Bi_x}(x) = E_{LH}^{GaAs} + \kappa x - P_\varepsilon + Q_{\varepsilon[100]} \quad (5)$$

where x is Bi composition, α and κ are the VCA contributions to the Bi-induced changes to the CB, and heavy hole (HH)/light hole (LH) bands, respectively. E_{CB}^{GaAs}, E_{HH}^{GaAs} and E_{LH}^{GaAs} are CB, HH and LH band edges of bulk GaAs, respectively. E_{HH}^{GaAs} and E_{LH}^{GaAs} are were taken as 0eV. While the localized Bi level is far from CB edge; it has been shown that Bi also affects the CB edge and α contains the effect of localised Bi level [24-26]. The value of κ is taken as 1.01eV and α is taken as 2.82eV [25]. a_{CB} is the hydrostatic deformation potential coefficient for CB. ε_{xx} and ε_{yy} are in-plane, and ε_{zz} is out-of plane strain parameters, which are defined as $\varepsilon_{xx} = \varepsilon_{yy} = [a_{GaAs} - a_{GaAs_{1-x}Bi_x}(x)]/a_{GaAs_{1-x}Bi_x}(x)$ and $\varepsilon_{zz} = -\left(\frac{2c_{12}}{c_{11}}\right)\varepsilon_{xx}$, where, a_{GaAs} and $a_{GaAs_{1-x}Bi_x}(x)$ are the lattice constants of GaAs and $GaAs_{1-x}Bi_x$, respectively. c_{11} and c_{12} are the elastic constants. P_ε and $Q_{\varepsilon[100]}$ describe the influence of strain component on the VB edges of GaAs, which are defined as

$$P_\varepsilon = a_{VB}\left(\varepsilon_{xx} + \varepsilon_{yy} + \varepsilon_{zz}\right) + \frac{b}{2}\left(\varepsilon_{xx} + \varepsilon_{yy} - 2\varepsilon_{zz}\right) \quad (6)$$

$$Q_{\varepsilon_{[100]}} = a_{VB}\left(\varepsilon_{xx} + \varepsilon_{yy} + \varepsilon_{zz}\right) - \frac{b}{2}\left(\varepsilon_{xx} + \varepsilon_{yy} - 2\varepsilon_{zz}\right) \quad (7)$$

where a_{VB} is the hydrostatic deformation potential coefficient for VB of GaAs and b is the axial deformation potential coefficient of GaAs.

To calculate the strain-induced modifications on the bandedges of the samples grown on (311)B GaAs substrate, $Q_{\varepsilon[100]}$ parameter should be replaced with parameters related to [311] direction as [26],

$$Q_{\varepsilon[311]} = Q_{\varepsilon[100]} + \frac{\beta}{54.74}\left(Q_{\varepsilon[111]} - Q_{\varepsilon[100]}\right) \quad (8)$$

where β is an angle between [100] and [111] directions as 25.2° and

$$Q_{\varepsilon[111]} = d_v\sqrt{3}\left(\frac{C_{11}+2C_{12}}{2C_{12}+C_{11}+4C_{44}}\right)\varepsilon_{xx} \quad (9)$$

d_v is deformation potential, and C_{44} is elastic constant for VB of GaAs.

The effect of localized Bi level on the VB edge of GaAs was determined using VBAC model. As a result of VBAC model, VB splits into two levels, E_+ and E_-, where E_+ represents the VB edge of GaAsBi [8,9,11]. By using VBAC model and Eqs. 4-5, HH and LH energies were determined as

$$E_{HH^+}^{GaAs_{1-x}Bi_x}(x) = \frac{1}{2}\left[E_{Bi} + E_{HH}^{GaAs_{1-x}Bi_x}(x) + \sqrt{\left(E_{Bi} - E_{HH}^{GaAs_{1-x}Bi_x}(x)\right)^2 + 4{C_{BiM}}^2 x}\right] \quad (10)$$

$$E_{LH^+}^{GaAs_{1-x}Bi_x}(x) = \frac{1}{2}\left[E_{Bi} + E_{LH}^{GaAs_{1-x}Bi_x}(x) + \sqrt{\left(E_{Bi} - E_{LH}^{GaAs_{1-x}Bi_x}(x)\right)^2 + 4{C_{BiM}}^2 x}\right] \quad (11)$$

where x is the Bi concentration, E_{Bi} is the isolated Bi impurity energy level below VB maximum (-0.183eV)[25]. C_{BiM} is the interaction term of the VB of the host material with isolated Bi impurity level. In Eqs. 10-11, the $E_{HH}^{GaAs_{1-x}Bi_x}$ and $E_{LH}^{GaAs_{1-x}Bi_x}$ expressions are given in Eqs. 4-5.

Optical transition energies in GaAsBi are calculated in two steps. First, the band profile of bulk (100) and (311) GaAsBi are calculated by using Eqs. 3-11 as depicted in Figure 2. Figure 2 represents the modification of GaAs band profile as an effect of Bi composition. The sketch in Figure 2 from left bulk (100)/(311) GaAs to right bulk (100)/(311) $GaAs_{1-x}Bi_x$ represents an evolution of the band profile from GaAs to $GaAs_{1-x}Bi_x$ considering all contributions (VCA,

strain and VBAC model) step by step. The final band profile in Figure 2 contains all contributions and gives the exact band profile of $GaAs_{1-x}Bi_x$.

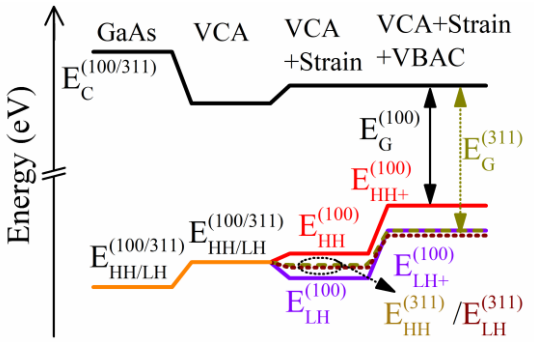

Figure 2. Modification of the band profile from bulk GaAs to bulk GaAsBi with depicting all contributions from VCA, strain and VBAC model. The final form of the sketch represents both band profiles of (100) and (311) GaAsBi.

At the second step, the quantized energy levels in GaAsBi QW are calculated by using finite QW approximation and CB, and VB discontinuities are obtained using Eqs. 3-11. In the calculations, the parameters were taken from Ref. [27] for GaAs and Ref. [28] for GaAsBi, except for the effective mass of samples grown on (311)B. Nötzel *et al.* and Batty *et al.* showed for high index substrate that HH effective mass of GaAs are strongly affected by the substrate orientation, whereas LH effective mass is almost unaffected. The HH effective mass at [111] direction is almost doubled as compared to [100] direction effective mass[29,30]. The effective mass at [311] direction can be estimated by averaging the effective mass values at [100] and [111] direction values. Since Bi composition in GaAsBi is quite low, we assume that VB characteristic of the GaAsBi is similar to that of GaAs. Therefore, the effective mass of (311)B oriented samples were calculated using effective masses of GaAs at [100] and [111] directions [29]. The parameters used in the calculations are given in Table I. Some parameters used in the calculations are unknown for GaAsBi alloys in the literature; therefore for unknown GaAsBi parameters, we considered parameters of GaAs [7].

Table I. The parameters used in the band alignment calculations. GaAs and GaAsBi parameters were taken from Ref. [27] and [28], respectively. Composition-dependent alloy parameters were obtained by using Vegard's law. The parameters for GaAs is used for the unknown parameters for GaAsBi, considering very low concentration of Bi in GaAs lattice.

Parameters (Unit)	$GaAs_{1-x}Bi_x$ (100)	$GaAs_{1-x}Bi_x$ (311)
a (A)	5.653+0.671x	
c_{11} (10^{11}dyne/cm^2)	12.21-4.91x	
c_{12} (10^{11}dyne/cm^2)	5.66-2.39x	
c_{44} (10^{11}dyne/cm^2)	6.00-5.637x	
a_{CB} (eV)	-7.17	
a_{VB} (eV)	1.16	
b (eV)	-2	
d_v (eV)	-4.8	
m_e (m_0)	0.067	
m_{hh}(m_0)	0.35	0.5349
m_{lh}(m_0)	0.082	

3. RESULTS AND DISCUSSION

3.1 HR-XRD Results

Figure 3 shows HR-XRD diffraction curves (2θ-ω scans) of two samples, whose HR-XRD results exhibit well-defined fringes around the sharp (100) and (311) diffraction peaks. This is an indication of a smooth interface between the epitaxial layer and substrate. The experimental diffraction curves were simulated by using dynamical scattering theory [31]. The best fits are shown as solid lines in Figure 3. We find the Bi contents as 2.15% and 2.10% for the GaAsBi QW layer of the samples grown on (100) and (311)B substrates, respectively. As seen in the inset of Figure 3, Bi composition is not limited in the QW layer, but spreads out from the GaAsBi QW, resulting in the formation of a GaAsBi epilayer. The thickness of the Bi-containing layers for both samples is much larger than the nominal GaAsBi QW thickness. Therefore, the Bi-containing layers behave like an epilayer, not exactly like a QW. Since the GaAs cap was grown at the same temperature with the GaAsBi QW, it can be thought that Bi atoms continue to move through GaAs cap layer. The thickness of the Bi-containing layers is almost the same for both sample; however, the amount of the Bi in the GaAs cap in the sample

grown on (311)B GaAs is higher. Referring to the obtained Bi composition distribution shown in the inset of Figure 3a and b, the calculated bandgap and subband energy levels of the samples grown on (100) and (311) GaAs is illustrated in Figure 4. The band alignment of the GaAsBi QW is type I as seen in Figure 4, according to our calculations. It is well-known that both low-temperature growth GaAs and GaAsBi contains localized levels [11,32]; therefore we also included the localized levels in the illustration of the band profile in Figure 4. It is worth noting that the localization energy levels are schematically represented, not calculated.

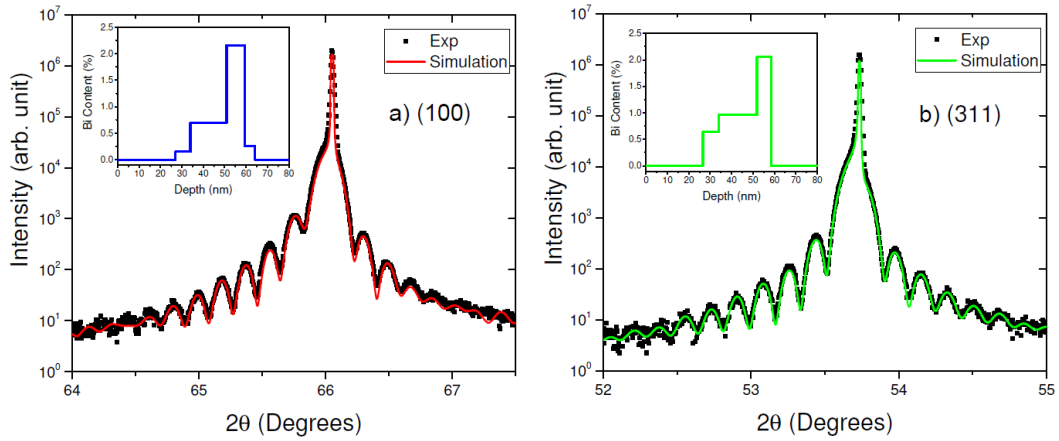

Figure 3. Experimental HR-XRD diffraction curves (■) of the samples grown on (a) (100) GaAs and (b) (311)B GaAs substrates. The corresponding simulations are depicted as solid lines. The corresponding Bi depth profiles starting from the GaAs cap layer towards to GaAs buffer layer are shown in the insets.

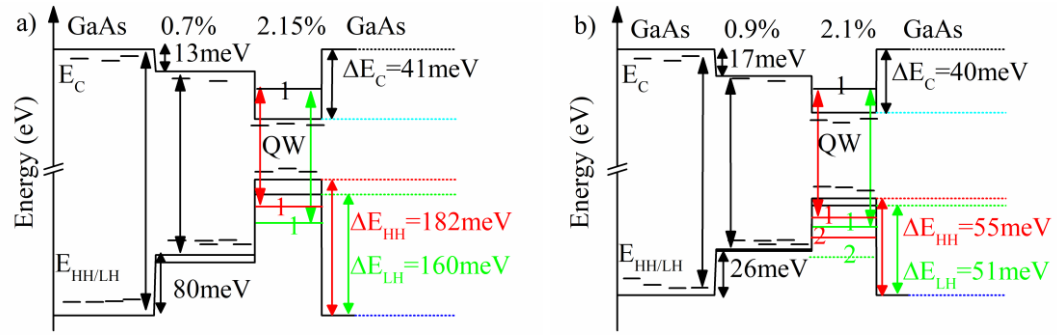

Figure 4. Calculated band profile and subband energies of the sample grown on (100) and (311) GaAs by using determined Bi composition profile shown in insets of Figure 3. The dashed black lines in the bandgap of the GaAs and GaAsBi represents localized levels. The black, red and green numbers in QW represent quantized energy level of CB, HH and LH, respectively. ΔE is ascribed for bandgap discontinuity.

Since we could not observe well-defined fringes in HR-XRD spectra of the other samples, the band alignment of the other samples was calculated by exploiting Bi composition obtained from TDFF analyzes of PR spectra given in the next subsection.

3.2 PR Results

Figure 5 shows experimental, and TDFF fitted PR spectra together with the MIR peaks of $GaAs_{1-x}Bi_x/GaAs$ QW structures with various Bi compositions grown on (100) and (311)B substrates.

The PR spectra are divided into two sections shown in Figure 5. The right part of the PR spectrum at higher energies separated with a hatched area is related to PR signal from GaAs layers. We first discuss the GaAs-related section of the PR results. The PR amplitude of GaAs is much higher than that of GaAsBi grown on (100) GaAs; therefore, GaAsBi-related PR part at the left side of the hatched area was multiplied with a factor higher than one for clarity. On the contrary, the PR amplitude of GaAs grown on (311) GaAs is comparable with that of GaAsBi. GaAs-related PR signal has two distinct transition peaks for all samples except for the one with 1.4% Bi composition. The peak energies are slight deviates to lower or higher energies than the ideal bandgap energy of GaAs. Because of low-temperature growth conditions, two peaks at slightly lower and higher energies than the ideal bandgap energy of GaAs have been reported for low-temperature growth GaAs [33]. Therefore, we believe that the peaks located at lower or higher energies originate from low-temperature growth top GaAs layer. We do not further discuss the GaAs-related PR spectrum since it is out of the scope of this paper.

To analyze GaAsBi-related peaks, we consider both GaAsBi epilayers due to the extended Bi composition out of QW toward to top GaAs layer and GaAsBi QW layer as shown in Figure 3. The TDFF-fitted PR and the calculated transition energies for (100) and (311)B GaAsBi/GaAs QW samples are given in Table II and Table III, respectively. By using the determined Bi compositions values from HR-XRD results, C_{BiM} parameter is found from TDFF-fitted PR spectrum for the samples with 2.15 and 2.10% Bi grown on (100) and (311)B GaAs, respectively. It is known that C_{BiM} does not depend on alloy composition; therefore we use the same C_{BiM} parameter in the calculations to calculate optical transitions energies and find Bi composition for the other four samples. The C_{BiM} parameter is found as 1.7eV for the

GaAsBi with 2.15% Bi composition grown on (100) GaAs substrate agrees with the recent values obtained for GaAsBi on (100) GaAs. [6,7,25,34]. C_{BiM} parameters is determined as 0.9eV for (311)B oriented samples, which are lower than the C_{BiM} value for the sample grown on (100) GaAs. The electronic bandstructure and surface atomic bonding environment of (311)B sample are different from conventional (100) GaAs materials, which change some properties of the materials such as atomic potential, effective mass and atomic interaction. It is worth pointing out that the (311)B plane consists of both (100) and (111) surfaces [29,30]. The (311)B surface terminates with As atoms having three dangling bonds along [311] direction on [100] and [111] direction. Therefore, (311)B surface is different from (100) surface which may account for the lower value of C_{BiM} (0.9eV) for (311)B oriented samples.

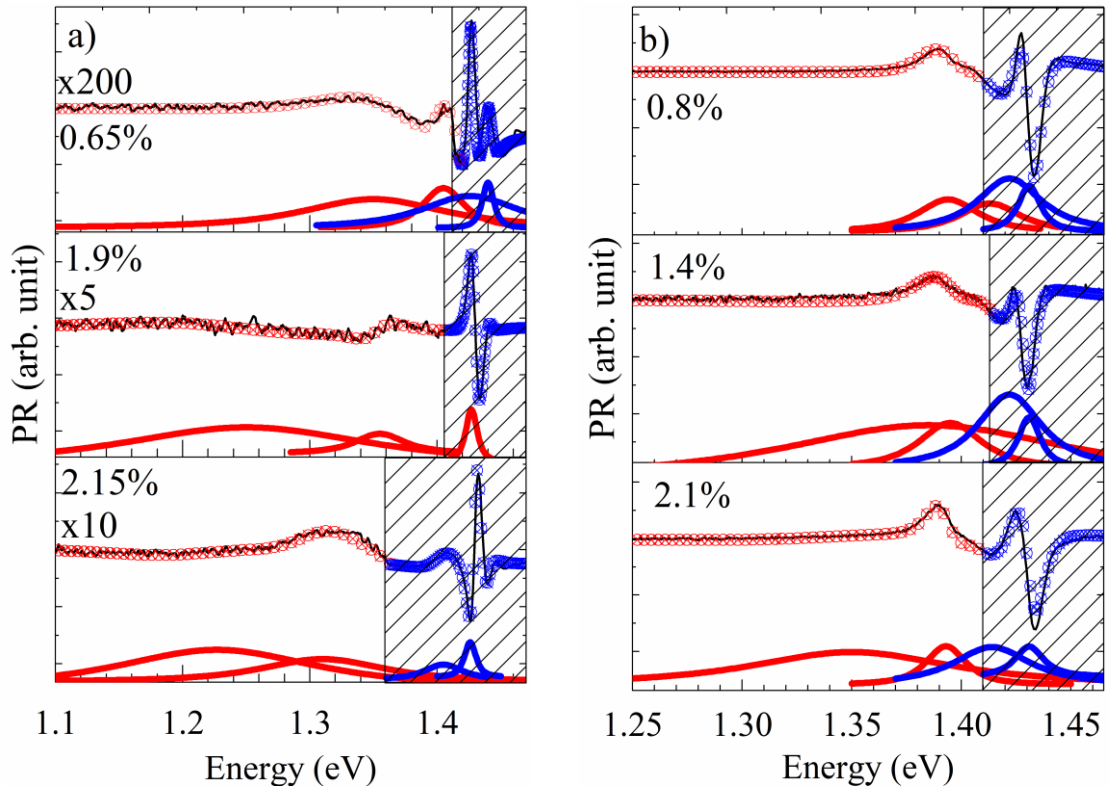

Figure 5. Experimental and TDFF-fitted PR with MIR spectra of $GaAs_{1-x}Bi_x$ ($0.0065 \leq x \leq 0.0215$) alloys grown on **a)** (100) and **b)** (311)B substrates. Black solid lines represent experimental results, and red and blue crossed-circle represent TDFF –fitted PR results of GaAsBi and GaAs layers, respectively. The MIR peaks are given below PR spectra. The hatched area is used to separate GaAs and GaAsBi layers PR signal. The results for the samples grown on (100) substrate are multiplied by a factor for clarity.

It is observed that the bandgap of GaAsBi decreases with increasing Bi concentration for all samples. The bandgap reduction of $GaAs_{1-x}Bi_x$ alloys obtained from TDFF fitting is approximately 92meV/%Bi and 36meV%Bi for samples grown on (100) and (311)B GaAs substrates, respectively. Since the C_{BiM} is a measure of the strength of the interaction between Bi level and GaAs CB, the less composition dependence of the bandgap of GaAsBi for (311) GaAsBi is attributed to the smaller C_{BiM} value.

As seen from Table II for the sample with 2.15% Bi composition grown on (100) GaAs substrates, the calculated E1-HH1 transition energy agrees with the TDFF-fitted PR results, whereas the calculated E1-LH1 transition energy of 1.27eV do not match with experimentally found 1.31eV transition energy. However, when we consider Figure 4a, it matches with the bandgap energy of 0.7%Bi containing GaAsBi epilayer; therefore this transition is ascribed to the bandgap of GaAsBi epilayer with 0.7% Bi composition in Table II. The bandgap of this epilayer is determined from bulk band edge energy of GaAs as formulated in Eqs 3-7.

It is evident that for all samples grown on (100) GaAs, the E1-HH1 transitions are matched with the TDFF fitted results, but the higher energy transitions do not match with the calculated E1-LH1 transition. Using the Bi compositions obtained from HR-XRD results, the higher energy transitions than E1-HH1 transitions are attributed to the bandgap energy of GaAsBi epilayers with 0.2%Bi and 0.5%Bi for 0.65%Bi and 1.9%Bi containing GaAsBi samples, respectively. However, considering that top GaAs layer is grown at low-temperature, the transition energy attributed to GaAsBi with 0.2%Bi composition may also arise from a localized level-related transition in GaAs. Furthermore, this transition cannot be ascribed for E1-LH1 since the line width of 1.405eV transition as 20meV is too narrow to include the E1-LH1 transition. Due to the uncertainty, a question mark is added in Table II for 0.65%Bi containing sample.

PR linewidth tends to increase with increasing Bi composition and the linewidth is broader compared to reported values [11,35,36], which can be related to the non-uniform Bi distribution in the samples as-well-as Bi-related localized states such as Bi pair, cluster and relatively low band-edge fluctuations [11,12].

Table II. Experimental and calculated energy values of the alloys grown on (100) oriented substrates. Tr. type and Loc. represent optical transition types and transition from localized level to the conduction band, respectively

%Bi	Exp. [eV]	Γ [meV]	C (10^{-9})	Calc. [eV]	Tr. type
2.15±0.05	1.227	120	10	1.225	E1-HH1
				1.27	E1-LH1
0.7±0.05	1.31	75	3.8	1.321	Epilayer
	1.405	23	6.76		GaAs
	1.426	6.3	2.6		GaAs
1.9±0.05	1.25	150	4.4	1.245	E1-HH1
				1.289	E1-LH1
0.5±0.05	1.355	30	0.045	1.353	Epilayer
	1.427	7	0.056		GaAs
0.65±0.02	1.355	85	5	1.352	E1-HH1
				1.38	E1-LH1
0.2 (?)	1.405	20	0.94	1.398	Epilayer/Loc.
	1.426	58	42		GaAs
	1.44	7	23.5		GaAs

As seen from Table III for 2.1%Bi containing sample grown on (311)B GaAs substrate, the TDFF fitted results match with the calculated E1-HH1, E1-LH1 and E1-HH2 transition energies. The HH and LH separation is quite small due to a lower strain effect on the band-edge compared to the samples results grown (100) substrate. Although E1-HH2 transition is forbidden in principle, it is possible to observe this transition in QW structures due to the broken crystal symmetry [37]. The three calculated transition energies are very close to each other; therefore cannot be separated at the PR spectrum due to broad line-width as 90meV According to optical transition calculation, the peak energy as 1.393eV may be ascribed for 0.9%Bi containing extended layer for 2.10%Bi containing samples. Moreover, considering low-temperature growth GaAs, the transition energy may also be ascribed to localized level-related transition. Due to this uncertainty, the question mark was added in Table III for 2.10%Bi containing samples. The similar results are obtained for the other samples. As for 0.8%Bi containing samples, 1.413eV transition energy may also be related to E1-HH2 transition in GaAsBi epilayer or localized level-related transition in low-temperature growth GaAs top layer.

Table III. Experimental and calculated energy value of the alloys grown on (311)B oriented substrates. Tr. type and Loc. represent optical transition types and transition from localized level to the conduction band, respectively

%Bi	PR [eV]	Γ [meV]	C (x10^{-9})	Calc. [eV]	Tr. type
				1.348	E1-HH1
2.1±0.05	1.35	90	10.7	1.364	E1-LH1
				1.362	E1-HH2
0.9(?)	1.393	14	0.3	1.383/1.393	Epilayer/Loc.
	1.414	24	12.5		GaAs
	1.431	9	3.3		GaAs
				1.376	E1-HH1
1.4±0.05	1.385	120	38	1.388	E1-LH1
				1.389	E1-HH2
0.6 (?)	1.395	22	1.8	1.395	Epilayer /Loc.
	1.419	18	13.14		GaAs
	1.429	6	2.15		GaAs
	1.394	21	1.67	1.399	E1-HH1
0.8±0.05				1.408	E1-LH1
	1.413	21	0.7	1.41	Epilayer/Loc.
	1.422	20	16		GaAs
	1.431	7	4		GaAs

A composition dependent characteristic of the quantized level sequence in QW is observed for the samples grown on (311)B GaAs substrate. Batty *et al.* [27] showed that the GaAs effective HH mass in GaAs/AlGaAs heterostructures is twice larger than that of (100) GaAs. Nötzel et al. reported for GaAs/AlAs that effective HH mass is larger at directions with higher Miller indices than at [100] [26]. This significant change in HH effective mass shifts the HH2 below LH1 quantized level in the QW for the 2.1%Bi containing (311)B oriented samples (see Table III). Since the strain effect on the band-edge of the (311)B samples is lower than the samples grown on (100) substrate, the separation of the HH1 and LH1 is smaller, which also contributes to facilitate HH2 level to move above LH1. As a conclusion, increasing Bi composition causes a change in the sequence of the quantized levels in the QW, which is not observed for the samples grown on (100) GaAs.

4. CONCLUSION

The composition dependence of the bandgap energy of GaAsBi grown on (100) and (311)B GaAs has been calculated with VBAC model, including strain–induced effect. The PR

transitions have been well fitted by the TDFF. Due to the strain effect and smaller effective mass values at [100], HH and LH quantized energy levels are well-separated from each other, and the only quantized E1-HH1 transition has been observed for the samples grown on (100) substrate. We have observed higher energy transition, E1-HH1, E1-LH1, E1-HH2, due to the smaller strain and higher effective mass values at [311] for the samples grown on (311)B. We have found that the effective bandgap energy decreases with increasing Bi concentration for all samples. PR linewidth tends to increase with Bi concentration for all (100) grown samples. We have observed a composition dependence of the quantized hole level sequence for the samples grown (311)B, that HH2 moves above LH1 for the sample with %2.1 Bi.

ACKNOWLEDGEMENTS

This work was partially supported by the Scientific Research Projects Coordination Unit of Istanbul University (ONAP-52321 and FYD-2016-20128) and supported by The Scientific and Technical Research Council of Turkey (TUBITAK) under Grant No. 115F063. YGG acknowledges the financial support from FAPESP (grants numbers 16/10668-7 and 14/50513-7).

JP, JH and MG acknowledge the financial support from European Research Council (ERC AdG AMETIST, #695116) and the Academy of Finland (TransPhoton, #259111).

REFERENCES

[1] Oe K and Okamoto H 1998 New Semiconductor Alloy GaAs1-xBix Grown by Metal Organic Vapor Phase Epitaxy *Jpn. J. Appl. Phys.* **37** L1283

[2] Yoshida J, Kita T, Wada O and Oe K 2003 Temperature Dependence of GaAs 1- x Bi x Band Gap Studied by Photoreflectance Spectroscopy *Jpn. J. Appl. Phys.* **42** 371

[3] Pettinari G, Polimeni A, Capizzi M, Blokland J H, Christianen P C M, Maan J C, Young E C and Tiedje T 2008 Influence of bismuth incorporation on the valence and conduction band edges of GaAs1−xBix *Appl. Phys. Lett.* **92** 262105

[4] Francoeur S, Seong M-J, Mascarenhas A, Tixier S, Adamcyk M and Tiedje T 2003 Band gap of GaAs1−xBix, 0<x<3.6% *Appl. Phys. Lett.* **82** 3874

[5] Fluegel B, Francoeur S, Mascarenhas a., Tixier S, Young E and Tiedje T 2006 Giant Spin-Orbit Bowing in GaAs1-xBix *Phys. Rev. Lett.* **97** 067205

[6] Usman M, Broderick C A, Lindsay A and O'Reilly E P 2011 Tight-binding analysis of the electronic structure of dilute bismide alloys of GaP and GaAs *Phys. Rev. B* **84** 245202

[7] Batool Z, Hild K, Hosea T J C, Lu X, Tiedje T and Sweeney S J 2012 The electronic band structure of GaBiAs/GaAs layers: Influence of strain and band anti-crossing *J. Appl. Phys.* **111** 113108

[8] Alberi K, Wu J, Walukiewicz W, Yu K M, Dubon O D, Watkins S P, Wang C X, Liu X, Cho Y-J and Furdyna J 2007 Valence-band anticrossing in mismatched III-V semiconductor alloys *Phys. Rev. B* **75** 045203

[9] Alberi K, Dubon O D, Walukiewicz W, Yu K M, Bertulis K and Krotkus A 2007 Valence band anticrossing in GaBixAs1−x *Appl. Phys. Lett.* **91** 051909
[10] Beaton D A, Mascarenhas A and Alberi K 2015 Insight into the epitaxial growth of high optical quality GaAs 1–x Bi x *J. Appl. Phys.* **118** 235701
[11] Mohmad A R, Bastiman F, Hunter C J, Richards R D, Sweeney S J, Ng J S, David J P R and Majlis B Y 2014 Localization effects and band gap of GaAsBi alloys *Phys. status solidi* **251** 1276
[12] Kudrawiec R, Syperek M, Poloczek P, Misiewicz J, Mari R H, Shafi M, Henini M, Gobato Y G, Novikov S V., Ibáñez J, Schmidbauer M and Molina S I 2009 Carrier localization in GaBiAs probed by photomodulated transmittance and photoluminescence *J. Appl. Phys.* **106** 023518
[13] Mooney P M, Watkins K P, Jiang Z, Basile A F, Lewis R B, Bahrami-Yekta V, Masnadi-Shirazi M, Beaton D A and Tiedje T 2013 Deep level defects in n-type GaAsBi and GaAs grown at low temperatures *J. Appl. Phys.* **113** 133708
[14] Look D C, Fang Z-Q, Sizelove J R and Stutz C E 1993 New AsGa Related Center in GaAs *Phys. Rev. Lett.* **70** 465–8
[15] Mohmad A R, Bastiman F, Hunter C J, Richards R, Sweeney S J, Ng J S and David J P R 2012 Effects of rapid thermal annealing on GaAs 1-x Bi x alloys *Appl. Phys. Lett.* **101** 012106
[16] Han X, Suzuki H, Lee J-H, Kojima N, Ohshita Y and Yamaguchi M 2011 N incorporation and optical properties of GaAsN epilayers on (311)A/B GaAs substrates *J. Phys. D. Appl. Phys.* **44** 015402
[17] Moto A, Takahashi M and Takagishi S 2000 Effect of Substrate Orientation on Photoluminescence of GaNAs *Jpn. J. Appl. Phys.* **39** L1267
[18] Henini M, Ibáñez J, Schmidbauer M, Shafi M, Novikov S V., Turyanska L, Molina S I, Sales D L, Chisholm M F and Misiewicz J 2007 Molecular beam epitaxy of GaBiAs on (311) B GaAs substrates *Appl. Phys. Lett.* **91**
[19] Kudrawiec R, Poloczek P, Misiewicz J, Shafi M, Ibáñez J, Mari R H, Henini M, Schmidbauer M, Novikov S V, Turyanska L, Molina S I, Sales D L and Chisholm M F 2009 Photomodulated transmittance of GaBiAs layers grown on (001) and (311)B GaAs substrates *Microelectronics J.* **40** 537
[20] Patil P K, Ishikawa F and Shimomura S 2016 GaAsBi/GaAs MQWs MBE growth on (411) GaAs substrate *Superlattices Microstruct.* **100** 1205
[21] Aspnes D E 1973 Third derivative modulation spectroscopy theory with low-field electroreflectance *Surf. Sci.* **37** 418
[22] Donmez O, Nutku F, Erol A, Arikan C M and Ergun Y 2012 A study of photomodulated reflectance on staircase-like, n-doped GaAs/AlxGa1-xAs quantum well structures. *Nanoscale Res. Lett.* **7** 622
[23] Hosea T J C 1995 Estimating critical point parameters of modulated reflectance spectra *Phys. Status Solidi B* **189** 531
[24] Pollak F H and Shen H 1993 Modulation spectroscopy of semiconductors: bulk/thin film, microstructures, surfaces/interfaces and devices *Mater. Sci. Eng. R Reports* **10** 374
[25] Broderick C A, Harnedy P E, Ludewig P, Bushell Z L, Volz K, Manning R J and O'Reilly E P 2015 Determination of type-I band offsets in GaBixAs1-xquantum wells using polarisation-resolved photovoltage spectroscopy and 12-band k.p calculations *Semicond. Sci. Technol.* **30** 94009
[26] Ibáñez J, Kudrawiec R, Misiewicz J, Schmidbauer M, Henini M and Hopkinson M 2006 Nitrogen incorporation into strained (In, Ga) (As, N) thin films grown on (100), (511), (411), (311), and (111) GaAs substrates studied by photoreflectance spectroscopy and high-resolution x-ray diffraction *J. Appl. Phys.* **100** 093522
[27] Vurgaftman I, Meyer J R and Ram-Mohan L R 2001 Band parameters for III–V compound semiconductors and their alloys *J. Appl. Phys.* **89** 5815
[28] Wang S Q and Ye H Q 2003 First-principles study on elastic properties and phase stability of III–V compounds *Phys. status solidi* **240** 45–54
[29] Nötzel R, Däweritz L and Ploog K 1992 Topography of high- and low-index GaAs surfaces *Phys. Rev. B* **46** 4736

[30] Batty W, Ekenberg U, Ghit A and O'Reilly E P 1989 Valence subband structure and optical gain of GaAs-AlGaAs (111) quantum wells *Semicond. Sci. Technol.* **4** 904–9
[31] Holý V, Pietsch U and Baumbach T 1999 *High-Resolution X-Ray Scattering from Thin Films and Multilayers* vol 149 (Berlin, Heidelberg: Springer Berlin Heidelberg)
[32] Dankowski S U, Kiesel P, Ruff M, Streb D, Tautz S, Keil U D, Sørensen C B, Knüpfer B, Kneissl M and Döhler G H 1997 Optical and electro-optical investigation of low-temperature grown GaAs *Mater. Sci. Eng. B* **44** 316–9
[33] Sinha S, Arora B M and Subramanian S 1996 Photoreflectance and photoluminescence spectroscopy of low-temperature GaAs grown by molecular-beam epitaxy *J. Appl. Phys.* **79** 427
[34] Donmez O, Kara K, Erol A, Akalin E, Makhloufi H, Arnoult A and Fontaine C 2016 Thermal annealing effects on optical and structural properties of GaBiAs epilayers: Origin of the thermal annealing-induced redshift in GaBiAs *J. Alloys Compd.* **686** 976–81
[35] Donmez O, Erol A, Arikan M C, Makhloufi H, Arnoult A and Fontaine C 2015 Optical properties of GaBiAs single quantum well structures grown by MBE *Semicond. Sci. Technol.* **30** 094016
[36] Fitouri H, Essouda Y, Zaied I, Rebey A and El Jani B 2015 Photoreflectance and photoluminescence study of localization effects in GaAsBi alloys *Opt. Mater. (Amst).* **42** 67–71
[37] Misiewicz J, Sitarek P and Sek G 2000 Photoreflectance spectroscopy of low-dimensional semiconductor structures *Opto-electronics Rev.* **8** 1